



Published in final edited form as:

*J Am Chem Soc.* 2008 July 23; 130(29): . doi:10.1021/ja801657y.

## Oxygen Reactivity of the Biferrous Site in the de novo Designed Four Helix Bundle Peptide DFsc: Nature of the “Intermediate” and Reaction Mechanism

Jennifer R. Calhoun<sup>†</sup>, Caleb B. Bell III<sup>||</sup>, Thomas J. Smith<sup>‡</sup>, Thomas J. Thamann<sup>§</sup>, William F. DeGrado<sup>\*†</sup>, and Edward I. Solomon<sup>\*</sup>

<sup>†</sup>Department of Biochemistry and Biophysics, School of Medicine, University of Pennsylvania, Philadelphia, Pennsylvania 19104-6059

<sup>‡</sup>Department of Chemistry, Kalamazoo College, Kalamazoo, Michigan 49006

<sup>§</sup>Pfizer Corp., Kalamazoo, Michigan 49001

<sup>||</sup>Department of Chemistry, Stanford University, Stanford, California 94305

Proteins containing carboxylate-bridged binuclear iron centers are members of a class of enzymes that activate dioxygen for subsequent oxidation and oxygenation chemistry.<sup>1</sup> Well-studied members of this superfamily are soluble methane monooxygenase (sMMO) that oxidizes methane to methanol,<sup>2</sup> the ribonucleotide reductase R2 subunit (R2) that generates a tyrosyl radical essential for the reduction of ribonucleotides to deoxyribonucleotides in DNA biosynthesis,<sup>3</sup> and stearyl-ACP<sup>9</sup> desaturase (<sup>9</sup>D)<sup>4</sup> that introduces a double bond into saturated fatty acids.<sup>5</sup> Despite differences in their overall structures and chemistry, dioxygen activation by these enzymes occurs at a nonheme diiron site that is supported by 2 histidines and 4 carboxylate ligands where, typically, a kinetically labile biferric-peroxo intermediate forms when O<sub>2</sub> reacts with the biferrous cofactor, followed by O–O bond cleavage and formation of high valent intermediates believed to be the reactive oxidants in at least MMO and R2. Despite these similarities, there are remarkable chemical differences among these enzymes. Understanding how these differences emerge and providing the basis for diverse catalytic pathways while preserving commonalities remains to be achieved. Furthermore the structures and the energetics of many of the intermediates and transition states within the catalytic cycles are controversial.<sup>6-8</sup>

To simplify and understand the mechanisms of enzymatic reactions at the diiron centers in a protein environment we have taken the approach of examining oxygen-activating reactions at the diiron center in our designed model system, the due ferri (DF) scaffold.<sup>9-16</sup> The DF scaffold is a simplified model of the natural enzymes, where the diiron site is housed within a four-helix bundle consisting of four carboxylate and two His ligands. Although our DF scaffold does not contain enzyme specific cofactor-tuning components, it has commonalities with the natural systems. Therefore, the reaction with ferrous ions and oxygen is expected to have functionally simplified properties that are common to the nonheme diiron carboxylate enzymes and can be used to identify properties that differentiate the members of this superfamily of enzymes from one another. The DF scaffold has the advantage over small

© 2008 American Chemical Society

\*wdegrado@mail.med.upenn.edu; edward.solomon@stanford.edu.

**Supporting Information Available:** Experimental methods, aerobic kinetics, 2-phase simulations to the anaerobic kinetic data and a low temperature CD/MCD spectrum of the DFscE11D oxidized species. This material is available free of charge via the Internet at <http://pubs.acs.org>.

molecule model complexes of reproducing the actual ligand set and sterically eliminating disproportionation of intermediates.

To explore O<sub>2</sub> reactivity with our de novo designed DF proteins, we start with the simplest reaction common with other diiron proteins, the ferroxidase reaction. In these substrate-independent reactions, the biferrous form of the enzymes react with O<sub>2</sub> to generate putative biferric  $\mu$ -hydroxo/oxo adducts. Herein we present the reactivity of the single chain DF protein (DFsc) and the coordinating amino acid variant DFscE11D. In previous studies of dimeric and tetrameric DF proteins we observed rapid formation of a biferric-oxo species that displays LMCT bands at 300 and 325 nm with extinction coefficients of 3240 and 2400 M<sup>-1</sup> cm<sup>-1</sup>, >respectively.<sup>10,14,15,17</sup> These values are in agreement with the ferroxidase sites of ferritin and other diiron proteins.<sup>18-21</sup> In the DFsc monomeric analogues the reaction of O<sub>2</sub> with either the Fe<sup>II</sup> preloaded or aerobically added produces a distinct species with a  $\lambda_{\text{max}}$  of 520 nm (19230 cm<sup>-1</sup>) (insets of Figure 1). Similarly species have occasionally been observed in some variants of previous designs in DF2 and DFtet.<sup>22</sup>

Kinetic studies showed that starting the reaction by addition of ferrous iron aerobically results in differences in the rate of formation of the 520 nm species between DFsc ( $t_{1/2} \approx 200$  s) and DFscE11D ( $t_{1/2} \approx 2200$  s); this reflects differences in iron loading kinetics between the variants (Figure S1). When Fe<sup>II</sup> is anaerobically preloaded into the peptides, rates of formation of the 520 nm species upon O<sub>2</sub> exposure are increased and within a factor of 2 of each other (vide infra). These differences in iron loading mask the actual reactivity of the cofactor site. Thus, the Fe preloaded complexes were chosen for further kinetic study.

The protein-iron complex was prepared anaerobically, and O<sub>2</sub>-saturated buffer was added to the biferrous complex, in a double-mixing stopped-flow reaction (Figure 1). A two phase model could not accurately reproduce the data (Figure S2). The observed kinetic behavior requires three phases (model shown in Figure 1) consisting of a formation phase and two subsequent phases. This model, where only B and C absorb at 520 nm (with the same extinction coefficient since full spectra taken near the beginning and end of the  $k_2$  phase overlay, Figure S3), well reproduces the observed kinetics. Parameters from this model that give realistic estimates for  $\epsilon_{520\text{nm}}$  are:  $k_1 = 2.1 \pm 0.1$ ,  $k_2 = 0.0049 \pm 0.0006$  and  $k_3 = 0.017 \pm 0.002$  s<sup>-1</sup> with  $\epsilon_{520\text{nm}} = 1213 \pm 25$  M<sup>-1</sup> cm<sup>-1</sup> (for both B and C) for DFsc, and  $k_1 = 4.4 \pm 0.3$ ,  $k_2 = 0.005 \pm 0.002$  and  $k_3 = 0.0029 \pm 0.0004$  s<sup>-1</sup> with  $\epsilon_{520\text{nm}} = 1043 \pm 16$  M<sup>-1</sup> cm<sup>-1</sup> (both B and C) for DFscE11D. The rate of formation is linearly dependent on O<sub>2</sub> concentration (up to saturation at 25 °C) and reflects O<sub>2</sub> reacting with the biferrous site which is directly comparable to the O<sub>2</sub> reactions of the binuclear nonheme iron enzymes. The  $k_3$  phase represents loss of the biferric cluster (produced in the O<sub>2</sub> reaction) from the peptide resulting in precipitated iron products. While the  $k_2$  phase may reflect relaxation of the DFsc scaffold subsequent to the formation of an Fe-O(phenolate) bond (vide infra), as this phase is lacking in a Y51 variant.<sup>23</sup>

The rates for the formation of the 520 nm species ( $k_1$ ) are 3 orders of magnitude faster than the rates of formation for the biferric-oxo bridge species in the A<sub>2</sub>B<sub>2</sub> DF systems<sup>24</sup> but similar to *E. coli* R2 (~1 s<sup>-1</sup>),<sup>25</sup> suggesting that the diiron site in DFsc is quite accessible to dioxygen and ready for rapid reaction. The 520 nm species formed in DFscE11D is more stable with respect to loss of Fe<sup>III</sup> (vide supra) and displayed more intense resonance Raman (rR) features enabling the absorption band to be profiled.

rR spectroscopy was used to characterize the 520 nm species in DFsc and DFscE11D (Figure 2). Both spectra, taken with 530 nm laser excitation, exhibit highly similar resonance enhanced vibrations (based on loss of these features in spectra taken off-resonance at 752 nm excitation). The intensity pattern and energy of the bands at 1178,

1279, 1502, and 1602  $\text{cm}^{-1}$  (labeled for DFscE11D in Figure 2) correlate well with  $\text{C-H}$ ,  $\text{C-O}$ ,  $\text{C-C}$ , and  $\text{C-C}$  modes, respectively, of a phenolate bound to  $\text{Fe}^{\text{III}}$ , and the features at 841 and 889  $\text{cm}^{-1}$  are assigned as a metal-coordinated tyrosyl Fermi doublet, frequently observed in the rR spectra from tyrosyl  $\text{Fe}^{\text{III}}$  charge transfer transitions in enzymes such as purple acid phosphatase and catechol 1,2-dioxygenase.<sup>26-28</sup> No isotope shift was observed for these features using either  $^{18}\text{O}_2$  or  $\text{H}_2^{18}\text{O}$  (data not shown) thus confirming that these vibrations are associated with coordination of a tyrosine residue producing a tyrosyl  $\text{Fe}^{\text{III}}$  CT. Since at low temperature the 520 nm species does not show a MCD signal (Figure S4) the oxidized site must be diamagnetic and consist of two antiferromagnetically coupled ferric ions. Thus oxidation of the biferrous DFsc cofactor site produces a tyrosine-bound biferric site.

In the diZn-DFsc NMR<sup>29</sup> structure two tyrosine residues (Y18 and Y51) are present in close proximity to the cofactor site. Therefore, in principle, either or both could coordinate terminally to a ferric center. Coordination of two to one iron or bridging would require extensive changes in the secondary structure of the peptide. Two resonance enhanced vibrations are observed at 563 and 587  $\text{cm}^{-1}$  (in the  $\text{O-Fe}^{\text{III}}$  stretch region) and one could derive from each  $\text{Fe-O(phenolate)}$  mode or both could be due to one  $\text{Fe-O(phenolate)}$  vibration split by Fermi resonance. To determine if one or two tyrosine residues are bound to the ferric centers in the oxidized species, the excitation profile of the 520nm band in DFscE11D was determined (inset Figure 2). The 563, 587, 1179 and 1278  $\text{cm}^{-1}$  modes all profile together across the absorption band in a manner consistent with only one phenolate to ferric CT. Therefore, upon exposure to dioxygen either Y18 or Y51, but not both, binds terminally to a ferric center at a biferric oxidized site. Preliminary results on DFsc variants show that Y51 is bound in the biferric state.<sup>23</sup>

These de novo designed preloaded cofactor sites react with  $\text{O}_2$  at a rate similar to that of the biferrous site of R2. However, the species formed is not an oxygen intermediate but an oxidized biferric site with one nearby tyrosine of the protein coordinated terminally. This indicates that while the initial reaction reduces  $\text{O}_2$  to a putative peroxide level intermediate, this is rapidly lost leaving a tyrosine coordinated, oxidized biferric site. Spectroscopic evidence shows that no tyrosine residue is coordinated in the biferrous state.<sup>23</sup> Thus phenol coordination to the oxidized site would provide a  $\text{H}^+$  to promote loss of  $\text{H}_2\text{O}_2$ , similar to the ferroxidase reaction observed in the early stage of the biferrous M-ferritin reaction with  $\text{O}_2$ . Studies are underway to further understand this reaction and to eliminate the appropriate tyrosine from the scaffold.

## Supplementary Material

Refer to Web version on PubMed Central for supplementary material.

## Acknowledgments

We are grateful for financial support by NSF-Biophysics Program Grant MCB-0342807 (E.I.S.) and NIH Grant GM54616 (W.F.D). We also thank Dr. Grit Straganz and Dr. James Lear for insightful discussions regarding these data and conclusions.

## References

- (1). Solomon EI, Brunold TC, Davis MI, Kemsley JN, Lee SK, Lehnert N, Neese F, Skulan AJ, Yang YS, Zhou J. *Chem. Rev.* 2000; 100:235–350. [PubMed: 11749238]
- (2). Merckx M, Kopp DA, Sazinsky MH, Blazyk JL, Muller J, Lippard SJ. *Angew. Chem., Int. Ed.* 2001; 40:2782–807.

- (3). Strand KR, Karlsen S, Kolberg M, Rohr AK, Gorbitz CH, Andersson KK. *J. Biol. Chem.* 2004; 279:46794–801. [PubMed: 15322079]
- (4). Lindqvist Y, Huang W, Schneider G, Shanklin J. *EMBO J.* 1996; 15:4081–92. [PubMed: 8861937]
- (5). Fox BG, Lyle KS, Rogge CE. *Acc. Chem. Res.* 2004; 37:421–9. [PubMed: 15260504]
- (6). Rinaldo D, Philipp DM, Lippard SJ, Friesner RA. *J. Am. Chem. Soc.* 2007; 129:3135–47. [PubMed: 17326634]
- (7). Murray LJ, Garcia-Serres R, Naik S, Huynh BH, Lippard SJ. *J. Am. Chem. Soc.* 2006; 128:7458–9. [PubMed: 16756297]
- (8). Krebs C, Galonic Fujimori D, Walsh CT, Bollinger JM Jr. *Acc. Chem. Res.* 2007; 40:484–92. [PubMed: 17542550]
- (9). Lear JD, DeGrado WF, Calhoun JR. *Proc Natl. Acad. Sci. U.S.A.* 2003; 100:14772–7. [PubMed: 14657351]
- (10). Pasternak A, Kaplan J, Lear JD, Degrado WF. *Protein Sci.* 2001; 10:958–69. [PubMed: 11316876]
- (11). Di Costanzo L, Wade H, Geremia S, Randaccio L, Pavone V, DeGrado WF, Lombardi A. *J. Am. Chem. Soc.* 2001; 123:12749–57. [PubMed: 11749531]
- (12). Calhoun JR, Kono H, Lahr S, Wang W, DeGrado WF, Saven JG. *J. Mol. Biol.* 2003; 334:1101–15. [PubMed: 14643669]
- (13). Cochran FV, Wu SP, Wang W, Nanda V, Saven JG, Therien MJ, Degrado WF. *J. Am. Chem. Soc.* 2005; 127:1346–7. [PubMed: 15686346]
- (14). Calhoun JR, Natri F, Maglio O, Pavone V, Lombardi A, Degrado WF. *Biopolymers.* 2005:264–78. [PubMed: 15700297]
- (15). Wei PP, Skulan AJ, Wade H, DeGrado WF, Solomon EI. *J. Am. Chem. Soc.* 2005; 127:16098–106. [PubMed: 16287296]
- (16). Wade H, Stayrook SE, Degrado WF. *Angew. Chem., Int. Ed. Engl.* 2006; 45:4951–4. [PubMed: 16819737]
- (17). Kaplan J, DeGrado WF. *Proc. Natl. Acad. Sci. U.S.A.* 2004; 101:11566–70. [PubMed: 15292507]
- (18). Yang YS, Baldwin J, Ley BA, Bollinger JM Jr. Solomon EI. *J. Am. Chem. Soc.* 2000; 122:8495–510.
- (19). Yang Y-S, Broadwater JA, Pulver SC, Fox BG, Solomon EI. *J. Am. Chem. Soc.* 1999; 121:2770–83.
- (20). Bollinger JM Jr. Tong WH, Ravi N, Huynh BH, Edmondson DE, Stubbe JA. *Methods Enzymol.* 1995; 258:278–303. [PubMed: 8524156]
- (21). Fox BG, Shanklin J, Ai J, Loehr TM, Sanders-Loehr J. *Biochemistry.* 1994; 33:12776–86. [PubMed: 7947683]
- (22). Marsh EN, DeGrado WF. *Proc. Natl. Acad. Sci. U.S.A.* 2002; 99:5150–4. [PubMed: 11959963]
- (23). Bell CB 3rd, Calhoun JR, Slonkina E, Wei PP, Hedman B, Hodgson KO, DeGrado WF, Solomon EI. Unpublished results.
- (24). Summa CM, Rosenblatt MM, Hong JK, Lear JD, DeGrado WF. *J. Mol. Biol.* 2002; 321:923–38. [PubMed: 12206771]
- (25). Tong WH, Chen S, Lloyd SG, Edmondson DE, Huynh BH, Stubbe J. *J. Am. Chem. Soc.* 1996; 118:2107–8.
- (26). Waldo GS, Theil EC. *Biochemistry.* 1993; 32:13262–9. [PubMed: 8241182]
- (27). Antanaitis BC, Streckas T, Aisen P. *J. Biol. Chem.* 1982; 257:3766–70. [PubMed: 7061509]
- (28). Gaber BP, Sheridan JP, Bazer FW, Roberts RM. *J. Biol. Chem.* 1979; 254:8340–2. [PubMed: 468828]
- (29). Calhoun JR, Liu W, Spiegel K, Dal Peraro M, Klein ML, Valentine KG, Wand AJ, DeGrado WF. *Structure.* 2008; 16:210–5. [PubMed: 18275812]

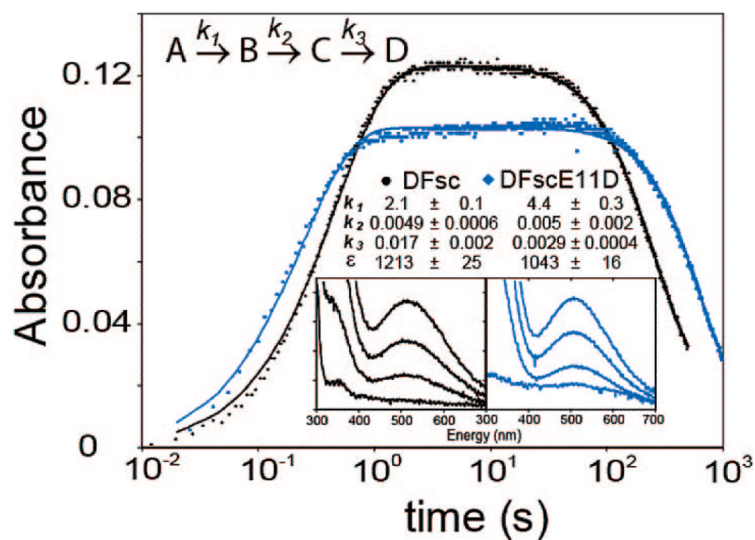


**Figure 1.**

Log of kinetics of O<sub>2</sub> reaction of biferrous loaded peptides. Reaction was monitored at 520 nm for DFsc (black) and DFscE11D (blue). Solid lines are three phase fits with parameters given in the text. Inserts show full spectrum development of the 520 nm band. Experimental details are given in the Supporting Information.

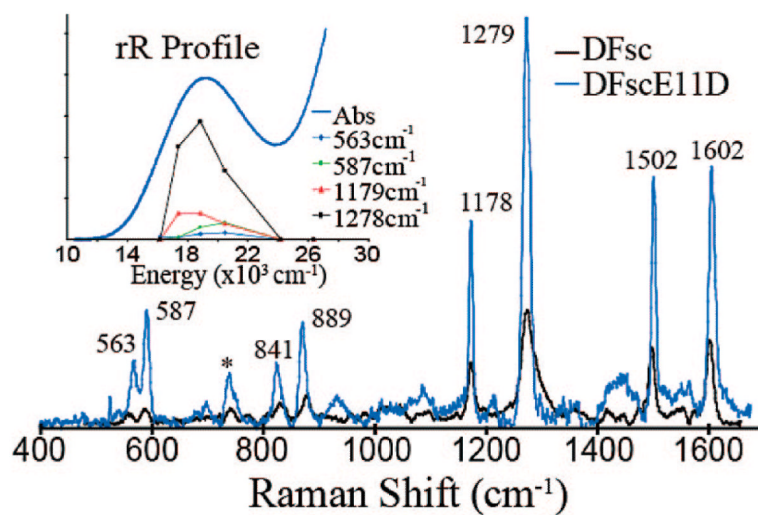


**Figure 2.** Resonance Raman spectra of O<sub>2</sub> reacted DFsc (black) and DFsc-E11D (blue). Spectra were obtained with 530 nm laser excitation and the specifics of experiment are in Supporting Information. Inset shows enhancement profiles for DFscE11D of the labeled features as a function of excitation energy.